Hindawi Publishing Corporation
Journal of Nanoscience
Volume 2014, Article ID 404519, 7 pages
http://dx.doi.org/10.1155/2014/404519

Research Article

Modulation of Carbon Nanotube Metal Contacts in Gaseous Hydrogen Environment

A. R. Usgaocar,[1] Harold M. H. Chong,[2] and C. H. de Groot[2]

[1] *Electrical and Computer Engineering, University of British Columbia, 341-2355 East Mall, Vancouver, BC, Canada V6T 1Z4*
[2] *School of Electronics and Computer Science, University of Southampton, Highfield, Southampton SO17 1BJ, UK*

Correspondence should be addressed to A. R. Usgaocar; ashwin.usgaocar@gmail.com

Received 31 December 2013; Accepted 1 March 2014; Published 27 March 2014

Academic Editor: Oleg I. Lupan

Carbon nanotubes (CNTs), contacted by electrodeposited $Pd_{0.59}Ni_{0.41}$ alloys, are characterised using electrical measurements and Raman spectroscopy. The high workfunctions of Nickel and Palladium form an ohmic contact with the CNT valence band, but the contact properties change on Hydrogen exposure due to a reduction in the PdNi workfunction and the realignment of the PdNi Fermi level with the CNT band structure. A PdNi contacted semiconducting CNT exhibited significantly lower currents after Hydrogen exposure while a metallic CNT exhibited a small current increase. The semiconducting and metallic natures of the CNTs are confirmed by their Raman spectra. This study demonstrates a technique for modulating the PdNi-CNT contact and differentiating between semiconducting and metallic CNTs via contact modulation. It also provides experimental evidence of the theoretical allocation of features in the CNT Raman spectra.

1. Introduction

Carbon nanotubes (CNTs), along with other carbon allotropes such as Graphene and Fullerenes, have sparked great interest in a multitude of research fields owing to their low dimensionality [1] and excellent electrical, mechanical, and thermal properties as well as high surface area to volume ratio [2]. The occurrence of metallic and semiconducting CNTs and demonstration of ballistic electron transport [3] have led to intense research into their use to further miniaturise electronic transistors, leading to all-Carbon circuits [4]. The ballistic electron transport also makes them an attractive material for spintronic devices [5], where electron spin is conserved by the absence of collision events. The high electronic conductivity and almost complete optical transparency of Graphene have led researchers to investigate its use as a transparent electrode [6] to replace the expensive Indium Tin Oxide (ITO). Innovative uses stemming from filling of hollow CNTs for use as battery anodes [7] and formation of high mechanical strength aerogels from Graphene [8] reveal the wide variety of applications possible with these versatile forms of Carbon.

Despite this promise, significant problems in production, positioning, and differentiation between metallic and semiconducting CNTs remain before individual CNT-based electronic devices become commercially viable. Studies that investigated the performance of transistors based on individual CNTs have found that the metal-CNT contacts play an important role in the device behaviour [9, 10]. The importance of metal-CNT contacts is further highlighted by Zhang et al. [11], who demonstrated a doping-free CNT transistor, controlled purely by the appropriate choice of metals to form electrical contacts. This makes the quality and nature of the metal-CNT junctions very important and also opens up potential applications that involve tuning the metal-CNT contacts through external stimuli.

CNTs exist in semiconducting as well as metallic form and it is necessary to distinguish between these two forms when they are used in device fabrication. One method for differentiation is via Raman spectroscopy and by studying the differences in specific features in the spectra. A second method is to use a CNT transistor and study the current variation during a large gate potential sweep (≈ -20 V to 20 V). Previous studies have used Raman [12, 13] and electrical

characterisation [3, 14], but results from using both these techniques on the same devices have not been reported.

Raman spectroscopy was used to independently differentiate between the metallic and semiconducting CNTs. The most important features of the Raman spectrum for CNTs are the Radial breathing mode (RBM), usually observed between 100 and 300 cm^{-1} and the G-band peaks observed between 1550 and 1590 cm^{-1} in the spectrum. A single CNT in resonance with the excitation laser produces a single RBM peak and a G-band that usually comprises two distinct peaks. The position of the higher wavenumber G-band peak is diameter independent while that of the RBM and the lower wavenumber G-band peak are diameter dependent, allowing diameter estimation using models described in the literature [13, 15]. In addition, the shape of the G-band peaks can also be used to differentiate between semiconducting and metallic CNTs. G-bands of semiconducting CNTs usually have two Lorentzian peaks at ≈1570 cm^{-1} and ≈1590 cm^{-1} while the metallic CNT G-bands have a Breit-Wigner-Fano (BWF) lineshape at ≈1550 cm^{-1} and one Lorentzian lineshape at ≈1590 cm^{-1} [13, 15]. Occasionally, metallic CNT G-bands exhibit a third Lorentzian peak at ≈1580 cm^{-1}, whose origin is unknown [13].

This paper describes the electrical characterisation of CNT transistors with electrodeposited PdNi contacts in air and Hydrogen ambients. Exposure to Hydrogen reduces the workfunctions of Pd/PdNi films, which changes the PdNi-CNT contact and allows more detailed differentiation of metallic and semiconducting CNTs. The nature of the CNTs is independently judged by using Raman spectroscopy and electrical characterisation on the same CNTs and the match between the two is examined. This is the first study that compares experimental results from electrical characterisation and Raman spectroscopy using the same CNTs.

2. Fabrication and Analytical Techniques

The CNTs used in this study were commercially sourced from Cheaptubes Inc., USA. A small amount of the CNT powder (<1 mg) was dispersed in 10 mL 1,2-dichlorobenzene by mixing and sonicating for 45 min. The sonicated solution was allowed to stand but no noticeable sedimentation was observed even over the course of weeks. The sonicated dispersion was filtered through a 2.5 μm filter paper to remove larger CNT aggregates and debris before spin coating the dispersion onto the substrate.

The substrate was an n-type ⟨100⟩, 1.39–1.41 Ω·cm Silicon wafer. A 20 nm insulating thermal oxide was grown on the Silicon to serve as the gate oxide. A 300 nm layer of Aluminium was evaporated on the back of the wafer and was followed by an anneal at 300°C to form an ohmic back contact. The CNT dispersion was spin coated onto the wafer using a standard resist spinner and was immediately followed by a layer of photoresist for the photolithography process and also to hold the dispersed CNTs in place. The contact patterns were defined by an EVG620TB mask aligner and the underlying thermal oxide in the windows was etched using buffered 20 : 1 HF. At the end of this step, the CNTs that bridge two contacts had their central section shielded by the photoresist and the CNT ends were exposed. The sample was then immersed in an electrochemical bath containing $NiSO_4$ and $Pd(en)Cl_2$ salts and the PdNi contacts were electrodeposited. The photoresist layer acts as an insulating layer to prevent electrodeposition on the CNTs. The PdNi alloy is deposited in the windows and forms end bonded contacts to the CNT, which are superior to the side bonded contacts [9]. Finally, the remnant photoresist is washed away using Acetone and Isopropyl alcohol (IPA) forming a three terminal transistor with the CNT as the channel.

For electrical characterisation, the devices were placed in the vacuum chamber of a Lakeshore EMTTP4 probe station and I-V measurements were performed using an Agilent 4155C semiconductor parameter analyser. The measurements in air ambient were performed without modifying the environment of the vacuum chamber in any way. The Hydrogen ambient measurements were performed by pumping down the vacuum chamber to ≈ 1.5×10^{-2} mbar, introducing pure Nitrogen till a base pressure of 0.3 bar and then a 5% Hydrogen/Nitrogen mixture till a partial pressure of 0.1 bar. This corresponds to a pure Hydrogen partial pressure of 5 mbar.

CNT transistors with electrodeposited contacts have a direct metal-substrate contact and can leak a large current through the substrate instead of the CNT. This leakage can be avoided with appropriate biasing if the metal-substrate junctions are Schottky diodes with low reverse bias currents. The electrodeposited PdNi-Si Schottky contacts were found to have very low reverse bias currents of a few nanoamperes and are favourable for suppressing the leakage current by maintaining the source and drain contacts at a lower potential than the back gate [16]. However, this also imposes the limitation that the gate voltage always has to remain positive compared to the drain and source to limit the leakage current.

3. Electrical and Raman Correlation

PdNi contacts were electrodeposited with varying separations to increase the likelihood of contacting the CNTs. Figure 1 shows SEM images of two such devices investigated in this study and Figure 2 shows the corresponding I-V characteristics in air and Hydrogen ambients. For easy reference, the devices shown in Figures 1(a) and 1(b) will be labelled as CNT 1 and CNT 2, respectively. The arrows marked in Figure 1 show the directions of the Raman scan discussed later in the paper. The currents measured in air for both devices are at least two orders of magnitude higher than typical reverse bias currents of PdNi-Si Schottky barriers and prove that the CNTs are connected to the source and drain contacts and carry most of the measured current.

The currents measured in air for both Devices 1 and 2 are similar to values recorded in previous studies using Pd contacted semiconducting CNTs [3]. While the current measured for CNT 2 (Figure 2(b)) in air is higher than that of CNT 1 (Figure 1(a)), it is still lower than those measured for Pd contacted metallic CNTs [17]. CNT 2 has a more ohmic characteristic, which suggests that the connecting

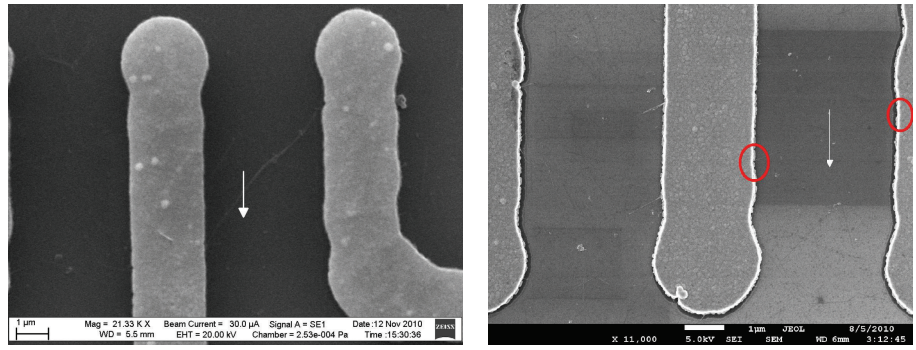

(a) (b)

Figure 1: SEM images of PdNi contacted CNTs. (a) CNT channel of CNT 1. (b) CNT channel of CNT 2. The CNT in (b) is parallel to the white line drawn in the figure. In both cases, the arrows show the direction of the Raman scan described later in the paper.

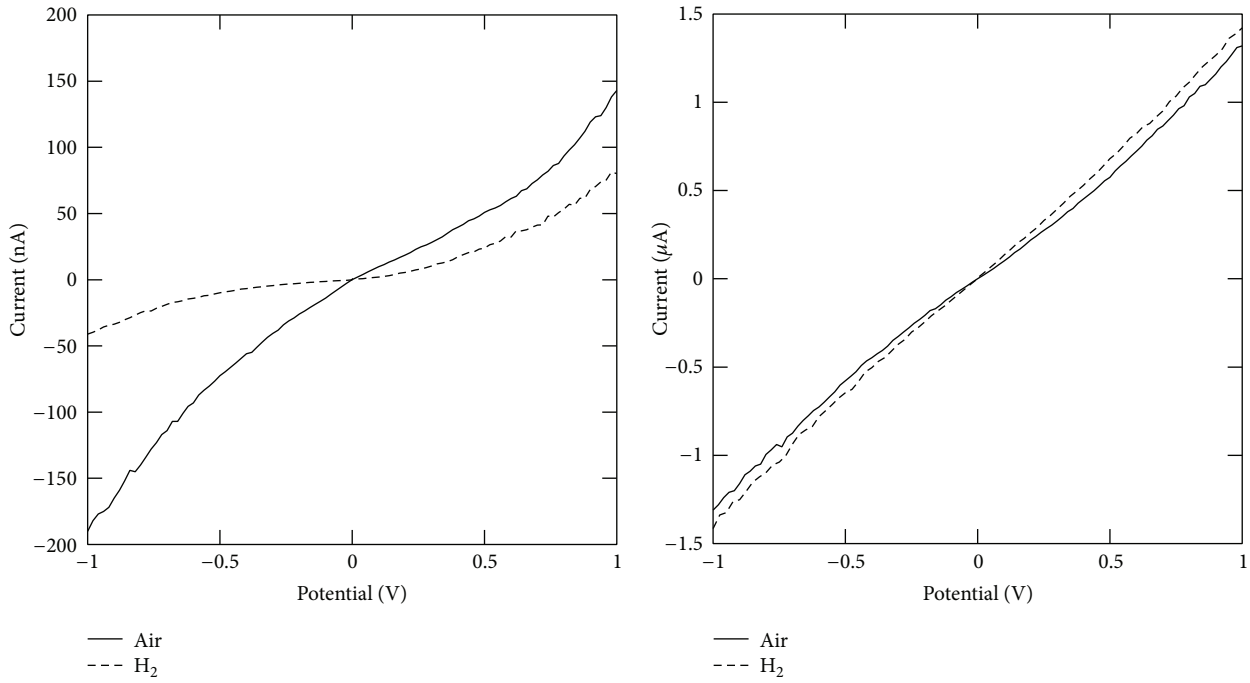

(a) (b)

Figure 2: I-V characteristics in air and Hydrogen of (a) CNT 1 with SEM image in Figure 1(a) and (b) CNT 2 with SEM image in Figure 1(b).

CNT is metallic. On the whole, an electrical characterisation in air without gate voltage variation is not conclusive in differentiating metallic and semiconducting CNTs.

The I-V characteristics of the two devices measured in a Hydrogen ambient provide more information about the nature of the CNTs. It is seen that a large percentage reduction is observed in the CNT 1 current on Hydrogen exposure, while that in CNT 2 shows a small percentage increase. These current changes can be explained by examining the effect of Hydrogen exposure on Pd contacted semiconducting and metallic CNTs.

It is well known that exposure of Pd/PdNi films to Hydrogen gas causes catalytic dissociation of Hydrogen molecules on the film surface. The dissociated Hydrogen atoms then diffuse into the PdNi films to form metal Hydrides, which have a lower workfunction compared to pristine PdNi [18, 19]. Figure 3(a) depicts the band diagram of the PdNi-semiconducting CNT contact with typical values of the PdNi workfunction and the CNT electron affinity. The CNTs are depicted as p-type in Figure 3(a) as previous studies describe their inherent p-type nature [14, 20]. In air, PdNi forms an ohmic contact with the CNT valence band that accounts for the nonrectifying characteristics of both devices in Figure 2. Exposure to Hydrogen changes the band structure to that shown in Figure 3(b) by reducing the PdNi workfunction and moving the PdNi Fermi level closer to the CNT valence band edge or possibly even into the bandgap. If the PdNi Fermi level remains inside the valence band, the

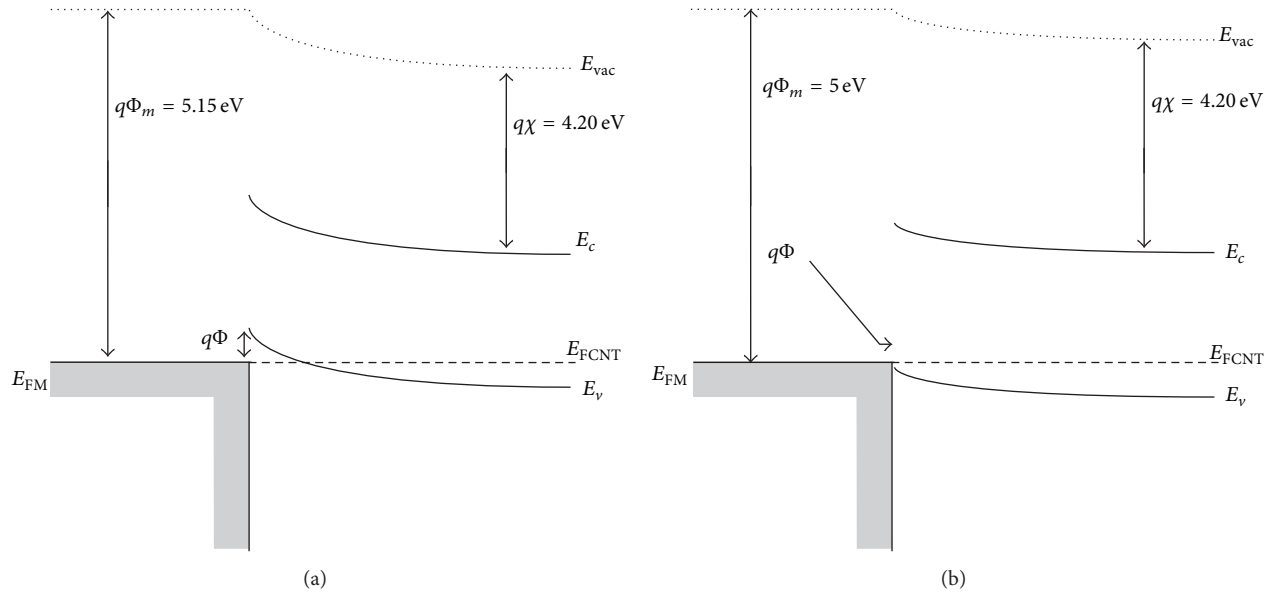

Figure 3: Band diagram of PdNi in contact with CNTs. (a) The band structure as formed in an air ambient. (b) Band structure after PdNi workfunction modification by Hydrogen exposure. On Hydrogen exposure, the PdNi Fermi level ($q\Phi_m$) decreases and changes the overlap between metal occupied states and CNT valence band edge ($q\Phi$), thereby modulating the metal-CNT contact.

current will decrease but the device retains its nonrectifying characteristics. On the other hand, if the Fermi level moves beyond the valence band and into the bandgap, a Schottky barrier will be formed between the PdNi and CNT and the device will assume a rectifying character. As metallic CNTs do not have a band gap, the device characteristics of a PdNi-metallic CNT should undergo no significant change on Hydrogen exposure.

Figure 2(a) shows a decrease in CNT 1 current but no transformation to rectifying character. The CNT 2 current in Figure 2(b) shows a slight increase in current on Hydrogen exposure. From these current changes and effect of Hydrogen on PdNi-CNT contacts described in Figure 3, it can be concluded that the CNT in CNT 1 is semiconducting while that in CNT 2 is metallic. As CNT 1 remained nonrectifying, it shows that the PdNi Fermi level has not moved into the CNT bandgap. The workfunction change was quantified by in situ measurement of the PdNi-Si Schottky barriers for both Devices 1 and 2 and shows a reduction of ≈150 mV. However, this value should be used with care as it does not account for the effect of Fermi level pinning in the PdNi-Si planar contact [21].

Raman spectroscopy was used to independently validate the conclusions from the electrical characterisation in air and Hydrogen. Raman spectra were measured at multiple points separated by 0.3 μm along the lines crossing the CNTs as shown in Figure 1. Figure 4(a) shows the G-band spectra for CNT 2 as the beam is swept across the CNT, with the individual spectra staggered along the intensity axis for clarity. This data shows the rise and fall of the intensity of the features as the laser spot is swept across the CNT, proving the presence of only one resonant CNT in the laser spot. Figure 4(b) shows the intensity of the RBM features for Devices 1 and 2 and also the strongest G-band feature of CNT 1, plotted as a function of the location on the scan line and staggered along the intensity axis. The lines in Figure 4(b) are Gaussian fits to the data and have full width half maximum values between 0.78 and 1.22 μm. This corresponds to a spot size consistent with the Raman spectrometer specifications of 1–3 μm. The Raman spectra for both Devices 1 and 2 had a single RBM peak with two distinct peaks in the G-band, as expected from a single CNT. The structure of the individual Raman spectra, in conjunction with the Gaussian distribution of intensity in Figure 4(b), proves the presence of a single resonant CNT in the laser spot for both of the devices.

Differences in the G-band lineshapes were used to classify the CNTs in the devices as semiconducting or metallic. The RBM and G-band of CNT 1 are shown in Figure 5 fitted with Lorentzian or BWF curves. The choice of these curves was primarily driven by their use in previous CNT studies [13, 15]. Gaussian fits to the data were also attempted but the fit quality was lower than or at most equal to that of the Lorentzian/BWF lineshapes. The RBM and G-bands of CNT 1 are shown in Figures 5(a) and 5(b), respectively, along with their fitted Lorentzian curves. The RBM peak is observed at 161 cm^{-1} and the G-band consists of two Lorentzian peaks at 1579 cm^{-1} and 1595 cm^{-1} which matches the pattern observed for semiconducting CNTs. The Raman spectra therefore independently validate the conclusion from the I-V characteristics that the CNT in this device is semiconducting. The diameter, calculated from the RBM and the lower frequency G-band peak [13], was 1.55 nm and 1.73 nm, respectively.

The RBM and G-band of CNT 2 are shown in Figures 6(a) and 6(b), respectively. An RBM peak is recorded at 183 cm^{-1} while the G-band consists of a BWF peak at 1552 cm^{-1} with

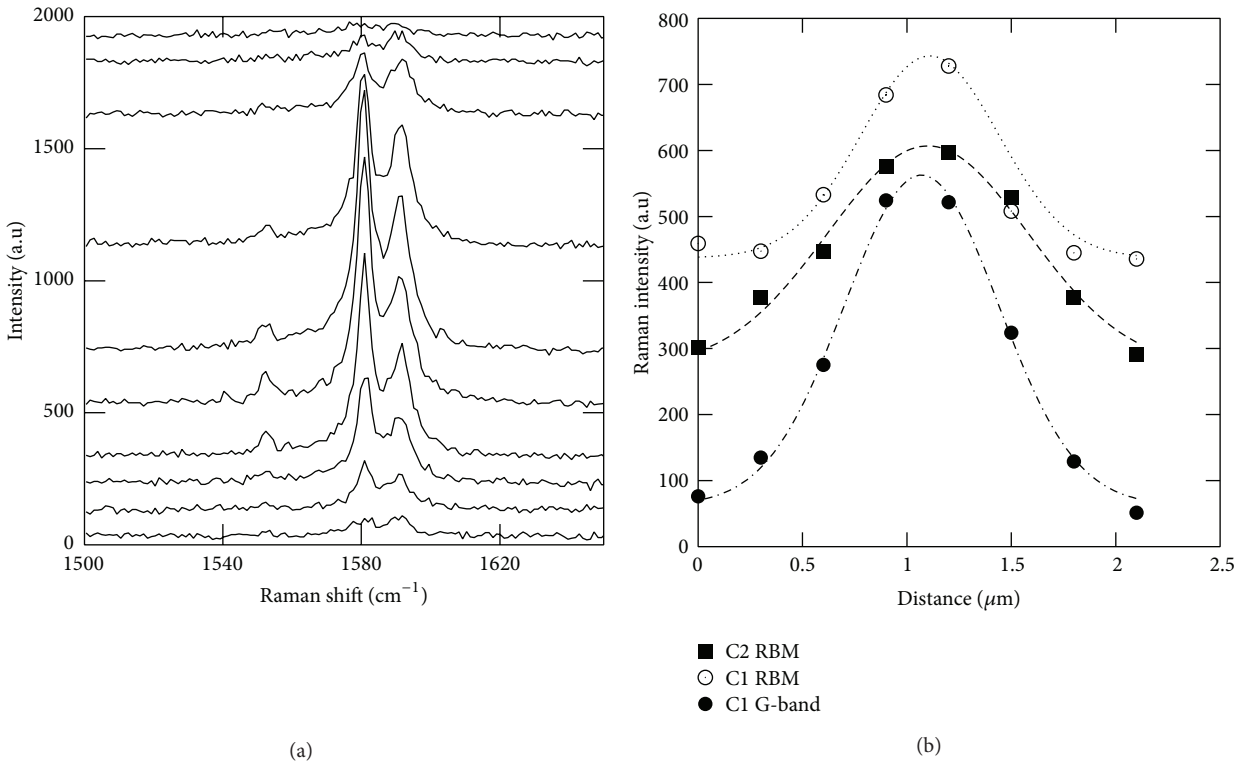

Figure 4: (a) Raman spectra showing the CNT 1 G-band. (b) Feature strengths of CNT 1 RBM (D1 RBM) and G-band (D1 G-band) and CNT 2 RBM (D2 RBM), measured at different points on the scan lines shown in Figure 1.

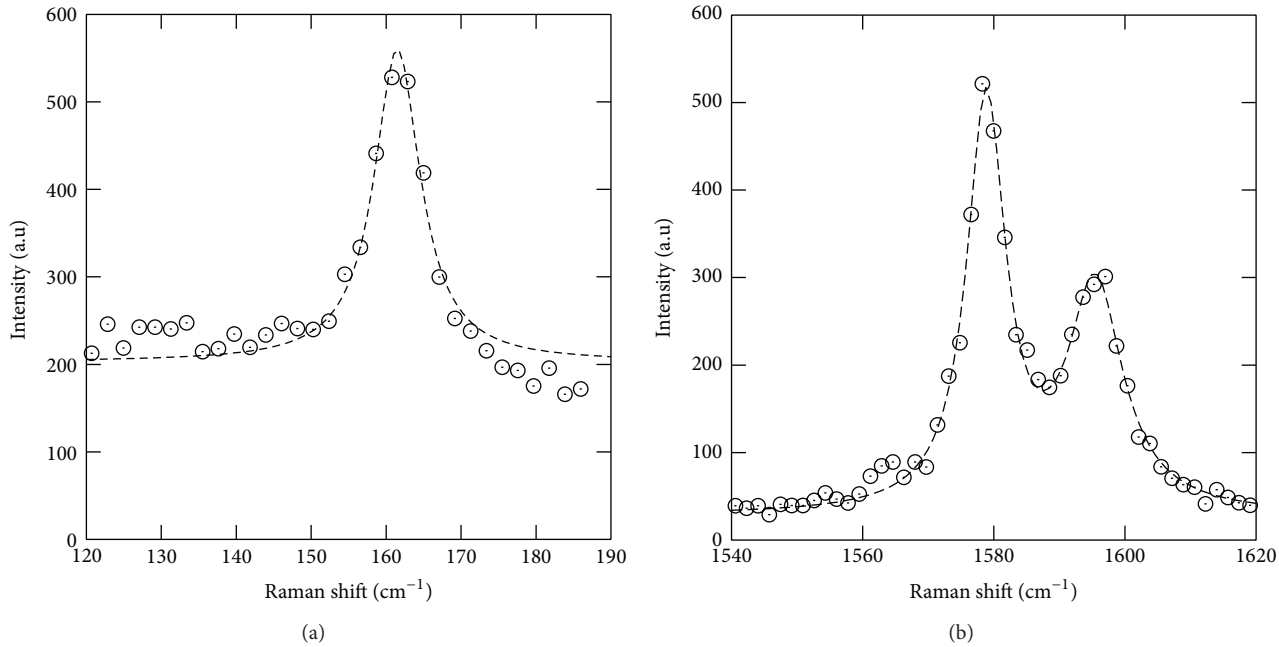

Figure 5: (a) The strongest RBM feature of the semiconducting CNT fitted with a Lorentzian curve. (b) The G-band of the CNT fitted with two Lorentzian curves. The points are the measured Raman data and the dashed line denotes the data fit.

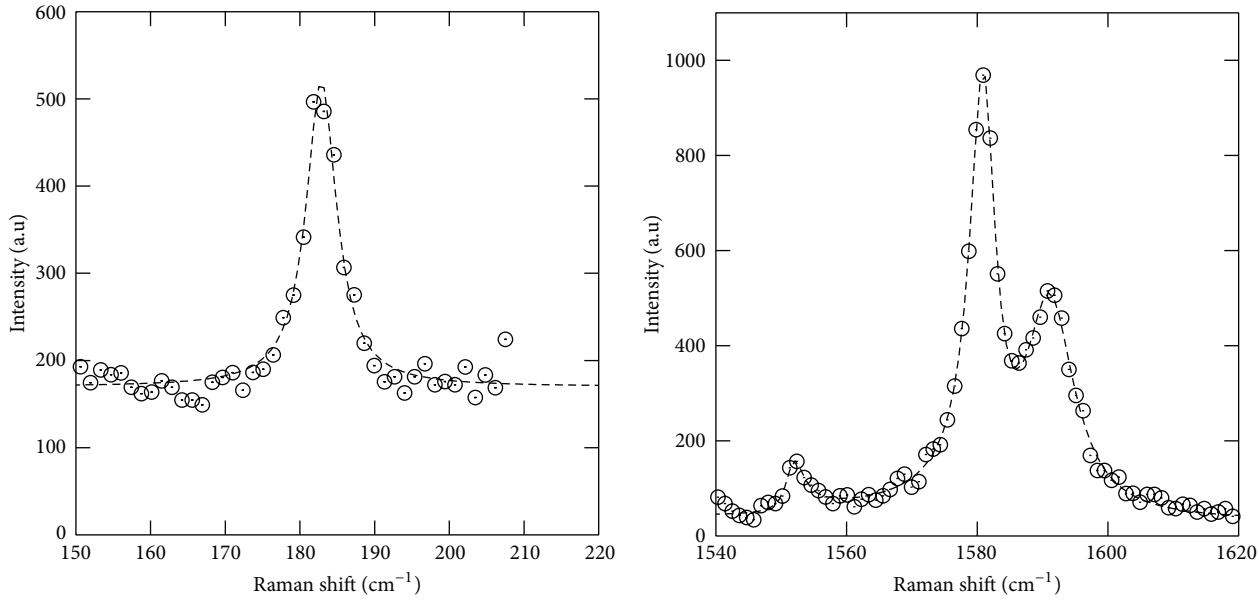

FIGURE 6: (a) The strongest RBM feature of the metallic CNT fitted with a Lorentzian curve. (b) The G-band of the CNT fitted with two BWF and one Lorentzian curves. The points are the measured Raman data and the dashed line denotes the data fit.

an asymmetry factor of 0.16 and two Lorentzian peaks at 1581 cm^{-1} and 1591 cm^{-1}. The G-band structure observed for this CNT has a good match with G-bands of metallic CNTs observed by Souza et al. [13] and therefore independently validates the conclusion from I-V characteristics that CNT 2 incorporates a metallic CNT. The CNT diameter, as calculated from the RBM and lower frequency G-band peak, is 1.36 nm and 1.43 nm, respectively.

The electrical and Raman spectroscopy results describe a method for differentiating between metallic and semiconducting CNTs by modification of the PdNi-CNT contacts using gaseous Hydrogen. It is observed that on exposure to Hydrogen, a large percentage decrease in current is measured in the device with PdNi-semiconducting CNT contacts. The device with PdNi-metallic CNT contact exhibits a small percentage increase in current and the reason for this increase is being investigated. The Raman spectra of both of these devices confirm the semiconducting and metallic nature of the CNTs and validate the results from the electrical characterisation.

4. Conclusions

The electrical and Raman spectroscopic characterisation of two transistors with electrodeposited PdNi contacts and CNT channels are presented. The electrical characterisations in air and Hydrogen ambients show that a marked decrease in the current through the CNT is observed in one transistor while a small current increase is observed in the second. Raman spectroscopy of the CNTs in the two transistors showed that these CNTs were semiconducting and metallic in nature, respectively. The resistance change for semiconducting CNT transistors is explained by the increase in the PdNi workfunction due to dissociation of Hydrogen on the film surface and diffusion of the Hydrogen atoms into the bulk of the film. To the best of our knowledge, this is the first study that experimentally demonstrates the match between electrical and Raman characterisation performed on the same CNT devices. Changing the workfunction of the metal contacts is equivalent to changing the metal itself as it actually changes the electron and hole barriers at the interface as against electrostatic coupling via a gate, which essentially modifies the energy bands in the bulk. Developing methods that revolve around such workfunction changes may create some valuable tools for studying metal-semiconductor interfaces.

Conflict of Interests

The authors declare that there is no conflict of interests regarding the publication of this paper.

References

[1] M. R. Buitelaar, A. Bachtold, T. Nussbaumer, M. Iqbal, and C. Schonenberger, "Multiwall carbon nanotubes as quantum dots," *Physical Review Letters*, vol. 88, Article ID 156801, 2002.

[2] R. Hu, B. A. Cola, N. Haram et al., "Harvesting waste thermal energy using a carbon-nanotube-based thermo-electrochemical cell," *Nano letters*, vol. 10, no. 3, pp. 838–846, 2010.

[3] A. Javey, J. Guo, Q. Wang, M. Lundstrom, and H. Dai, "Ballistic carbon nanotube field-effect transistors," *Nature*, vol. 424, no. 6949, pp. 654–657, 2003.

[4] X. Liang, S. Wang, X. Wei et al., "Towards entire-carbon-nanotube circuits: the fabrication of single-walled-carbon-nanotube field-effect transistors with local multiwalled-carbon-nanotube interconnects," *Advanced Materials*, vol. 21, no. 13, pp. 1339–1343, 2009.

[5] A. Cottet, T. Kontos, S. Sahoo et al., "Nanospintronics with carbon nanotubes," *Semiconductor Science and Technology*, vol. 21, no. 11, article S11, pp. S78–S95, 2006.

[6] J. O. Hwang, J. S. Park, D. S. Choi et al., "N-doped reduced graphene transparent electrodes for high-performance polymer light-emitting diodes," *ACS Nano*, vol. 6, no. 1, pp. 159–167, 2012.

[7] H. Zhang, H. Song, X. Chen, J. Zhou, and H. Zhang, "Preparation and electrochemical performance of SnO_2@carbon nanotube core-shell structure composites as anode material for lithium-ion batteries," *Electrochimica Acta*, vol. 59, pp. 160–167, 2012.

[8] M. Mecklenburg, A. Schuchardt, Y. K. Mishra et al., "Aerographite: ultra lightweight, flexible nanowall, carbon microtube material with outstanding mechanical performance," *Advanced Materials*, vol. 24, pp. 3486–3490, 2012.

[9] P. Avouris, "Molecular electronics with carbon nanotubes," *Accounts of Chemical Research*, vol. 35, no. 12, pp. 1026–1034, 2002.

[10] Z. Chen, J. Appenzeller, J. Knoch, Y. m. Lin, and P. Avouris, "The role of metal-nanotube contact in the performance of carbon nanotube field-effect transistors," *Nano Letters*, vol. 5, no. 7, pp. 1497–1502, 2005.

[11] Z. Zhang, X. Liang, S. Wang et al., "Doping-free fabrication of carbon nanotube based ballistic CMOS devices and circuits," *Nano Letters*, vol. 7, no. 12, pp. 3603–3607, 2007.

[12] M. S. Dresselhaus, A. Jorio, A. G. Souza Filho, G. Dresselhaus, and R. Saito, "Raman spectroscopy on one isolated carbon nanotube," *Physica B: Condensed Matter*, vol. 323, no. 1–4, pp. 15–20, 2002.

[13] F. Souza, A. Jorio, G. Dresselhaus et al., "Effect of quantized electronic states on the dispersive Raman features in individual single-wall carbon nanotubes," *Physical Review B—Condensed Matter and Materials Physics*, vol. 65, no. 3, Article ID 035404, pp. 354041–354046, 2002.

[14] R. Martel, T. Schmidt, H. R. Shea, T. Hertel, and P. Avouris, "Single- and multi-wall carbon nanotube field-effect transistors," *Applied Physics Letters*, vol. 73, no. 17, pp. 2447–2449, 1998.

[15] M. S. Dresselhaus, G. Dresselhaus, R. Saito, and A. Jorio, "Raman spectroscopy of carbon nanotubes," *Physics Reports*, vol. 409, no. 2, pp. 47–99, 2005.

[16] A. R. Usgaocar and C. H. de Groot, "Electrodeposited PdNi as possible ferromagnetic contacts for carbon nanotubes," *Physica Status Solidi B: Basic Research*, vol. 247, no. 4, pp. 888–891, 2010.

[17] D. Mann, A. Javey, J. Kong, Q. Wang, and H. Dai, "Ballistic transport in metallic nanotubes with reliable pd ohmic contacts," *Nano Letters*, vol. 3, no. 11, pp. 1541–1544, 2003.

[18] C. Weichsel, O. Pagni, and A. W. R. Leitch, "Electrical and hydrogen sensing characteristics of Pd/ZnO Schottky diodes grown on GaAs," *Semiconductor Science and Technology*, vol. 20, no. 8, pp. 840–843, 2005.

[19] T.-H. Chou, Y.-K. Fang, Y.-T. Chiang, C.-I. Lin, and K.-C. Lin, "Improving hydrogen detecting performance of a Pd/n-LTPS/glass thin film Schottky diode with a TiO_2 interface layer," *Sensors and Actuators B: Chemical*, vol. 134, no. 2, pp. 539–544, 2008.

[20] V. Derycke, R. Martel, J. Appenzeller, and P. Avouris, "Controlling doping and carrier injection in carbon nanotube transistors," *Applied Physics Letters*, vol. 80, no. 15, pp. 2773–2775, 2002.

[21] E. H. Rhoderick, "metal-semiconductor contacts," *IEE Proceedings I: Solid State and Electron Devices*, vol. 129, no. 1, pp. 1–14, 1982.